Science Advances
AAAS

Supplementary Materials for

Ketogenic diet uncovers differential metabolic plasticity of brain cells

Tim Düking *et al.*

Corresponding author: Gesine Saher, saher@mpinat.mpg.de

Sci. Adv. **8**, eabo7639 (2022)
DOI: 10.1126/sciadv.abo7639

The PDF file includes:

Figs. S1 to S7
Legends for tables S1 to S11
Legend for movie S1

Other Supplementary Material for this manuscript includes the following:

Tables S1 to S11
Movie S1

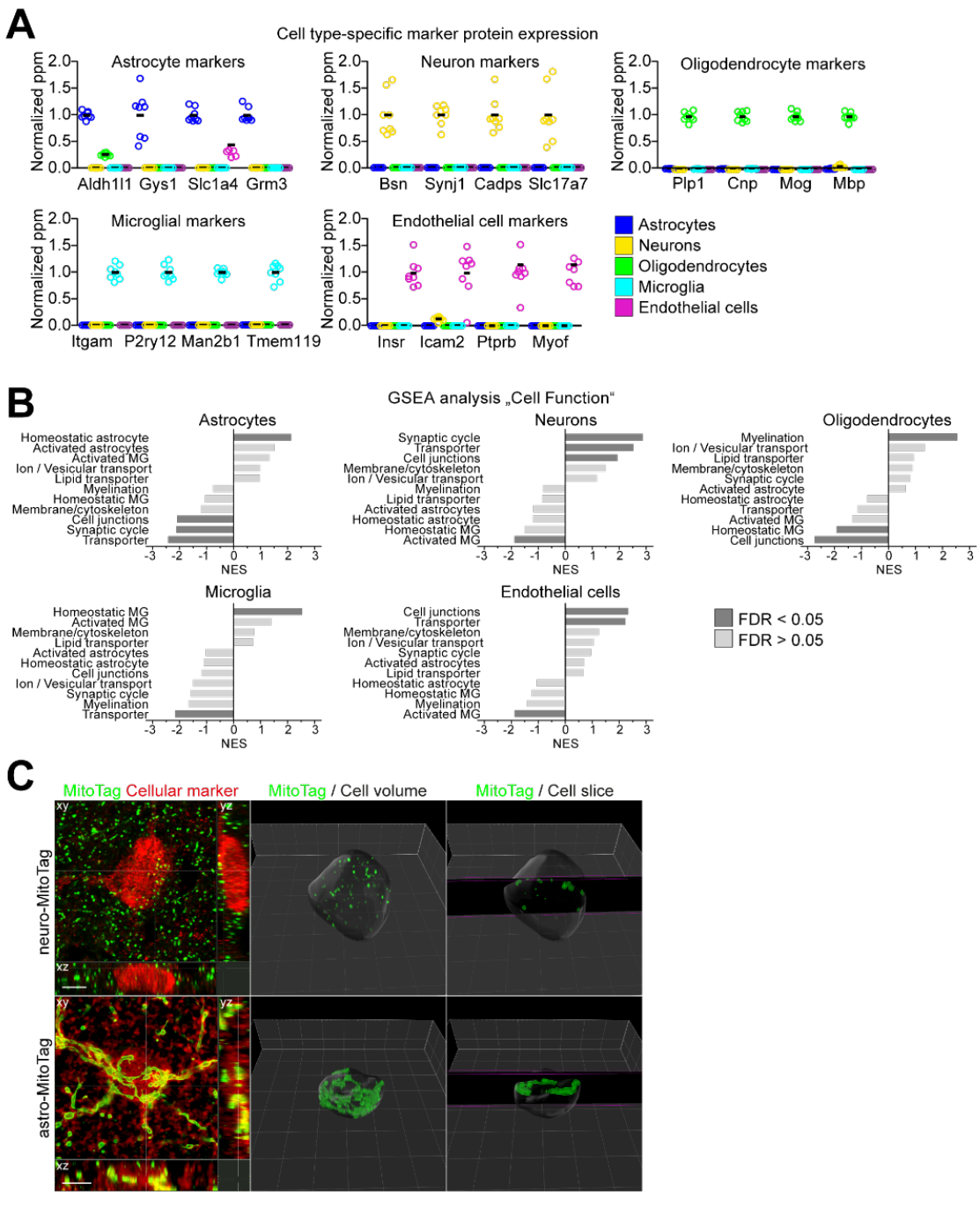

Fig. S1.

Proteome analysis of acutely isolated cortical cell types

(A) Mean relative abundance of selected marker proteins with individual values confirms cell type-specific enrichment of proteins. Shown are normalized ppm of selected marker genes across the 5 cell type fractions isolated from cortex of P42 mice.

(B) Normalized enrichment scores (NES) of gene sets 'cell function' by GSEA, comparing z-scores of cell type-specific proteomes from P42 mice (FDR, false discovery rate).

(C) Representative images of brain sections immunolabeled for astrocytes (3PDGH, red) or neurons (NeuN, red), and mitochondria (GFP, green) in the respective MitoTag transgenic mice (GFAP-Cre*MitoTag or Rbp4*MitoTag), showing maximum intensity projections (1 µm optical section in all dimensions, left panel). Cell soma surfaces were generated from

cellular immunolabeling (middle panel), from which mitochondria volumes and cell soma volumes were calculated. Optical sections (1 µm thickness) illustrate the cell type-specific mitochondria density (right panel). Scales, 5 µm.
FDR, false discovery rate; NES, normalized enrichment score.

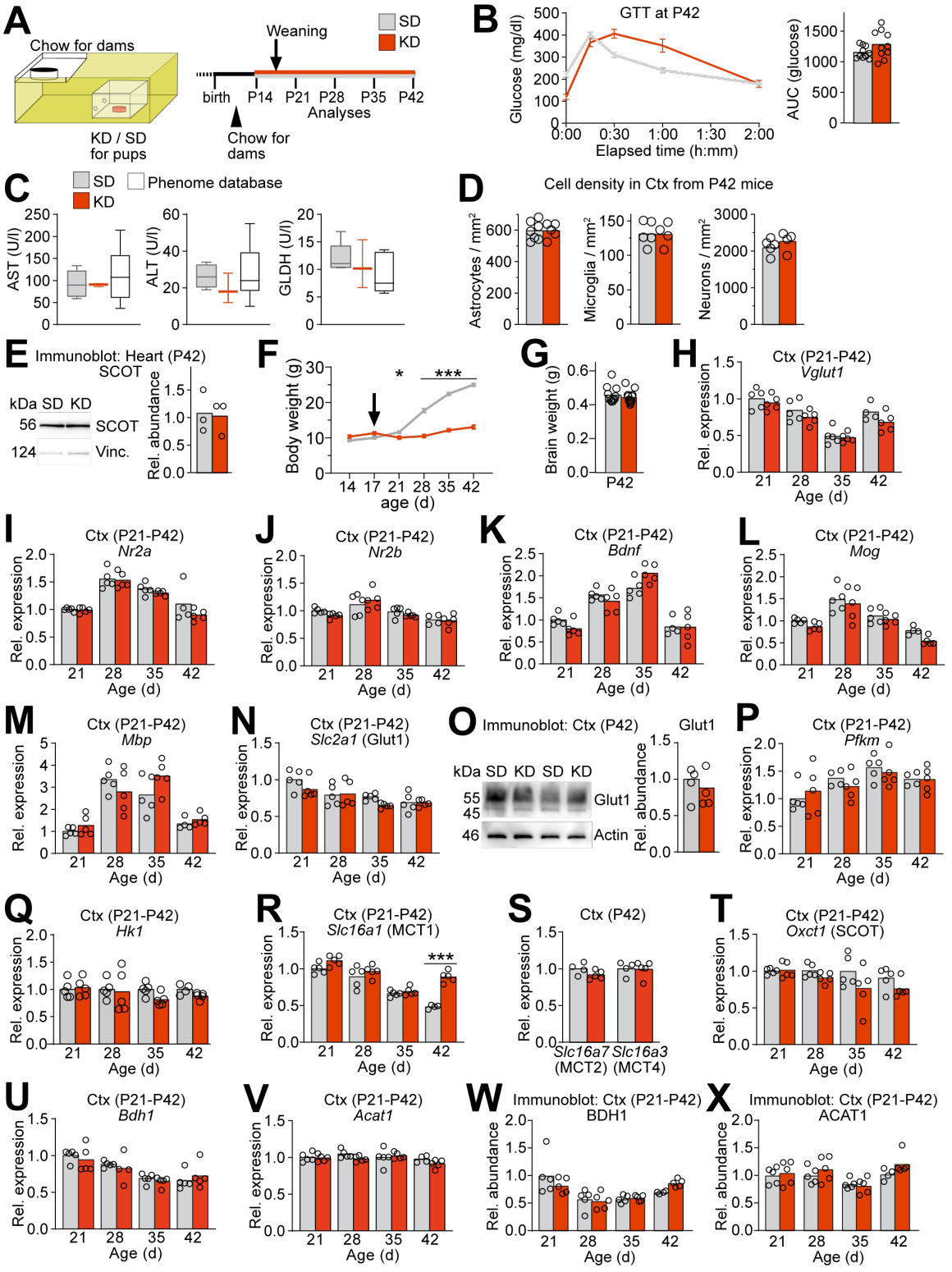

Fig. S2.

Cortical changes in mice weaned to a ketogenic diet

(A) Experimental setup. At postnatal day P10, normal chow for dams was replaced by liquefied powdered chow that was provided on an elevated shelf. At P14, normal chow (SD) or ketogenic diet (KD) was administered in boxes with small holes rendering this food only accessible for pups. Mice were weaned at P17 (arrow) and kept on the respective diet. Analyses were done at indicated ages.

(B) Glucose tolerance test (GTT) of P42 mice fed KD or SD with quantification of the area under the curve (n=10 animals per group).
(C) Activity of AST (aspartate transaminase), ALT (alanine transaminase), and GLDH (glutamate dehydrogenase) in serum from mice fed SD (n=5-7) or KD (n=3) in comparison to published reference intervals (Jackson laboratory mouse phenome database).
(D) Mean density of immunolabeled astrocytes (3PGDH), microglia (Iba1), and neurons (NeuN) with individual data points quantified on cortex sections from P42 mice fed KD or SD (n=4-6 mice per group).
(E) Representative immunoblot for SCOT at six weeks of age in heart tissue of mice fed SD or KD with quantification of mean relative abundance with individual data points. Reprobing for vinculin (Vinc.) confirmed equal protein loading (n=3 mice).
(F) Mean body weight of mice fed KD or SD (n=20, 2way ANOVA with Sidak's post test, ***$p<0.001$).
(G) Mean brain weight at P42 in mice fed SD or KD (n=12 mice).
(H) - (N) Mean cortical mRNA expression relative to P21 SD values with individual data points in mice fed SD or KD at indicated ages (n=4-5 mice), evaluating *Vglut1* (H), *Nr2a* (I), *Nr2b* (J), *Bdnf* (K), *Mog* (L), *Mbp* (M), and *Slc2a1* (N).
(O) Representative immunoblot for GLUT1 at six weeks of age in cortex of mice fed SD or KD with quantification of mean relative abundance with individual data points. Reprobing for actin confirmed equal protein loading (n=4 mice).
(P) - (R) Mean cortical mRNA expression relative to P21 SD values with individual data points in mice fed SD or KD at indicated ages (n=4-5 mice), evaluating *Pfkm* (P), *Hk1* (Q), and *Slc16a1* (R) (2way ANOVA with Sidak's post test, ***$p<0.001$).
(S) Mean cortical mRNA expression with individual data points in P42 mice fed SD or KD at indicated ages (n=4-5 mice), evaluating *Slc16a7* (MCT2) and *Slc16a3* (MCT4).
(T) - (V) Mean cortical mRNA expression relative to P21 SD values with individual data points in mice fed SD or KD at indicated ages (n=4-5 mice), evaluating *Oxct1* (SCOT) (T), *Bdh1* (U), and Acat1 (V).
(W) - (X) Mean protein abundance relative to P21 SD values with individual data points in immunoblots probed for BDH1 (W), and ACAT1 (X) (n=5 mice). Data were normalized to reprobed actin signals.

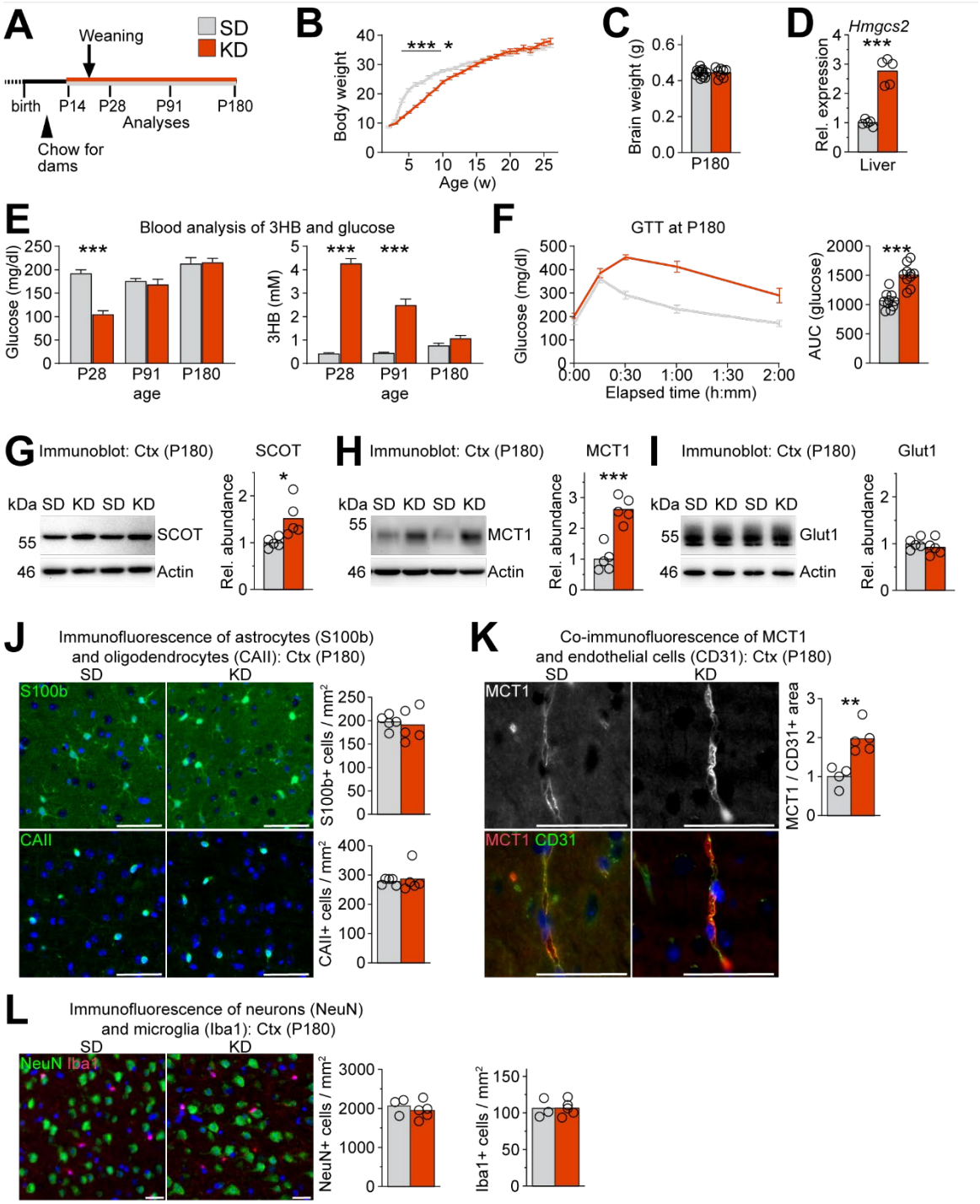

Fig. S3.

Phenotyping of mice after long-term feeding with ketogenic diet

(A) Experimental setup. At postnatal day P10, normal chow for dams was replaced by liquefied powdered chow that was provided on an elevated shelf. At P14, normal chow (SD) or ketogenic diet (KD) was administered in boxes with small holes rendering this food only accessible for pups. Mice were weaned at P17 (arrow) and kept on the respective diet. Analyses were done at indicated ages.

(B) Mean body weight of mice fed KD or SD (n=24-25, 2way ANOVA with Sidak's post test, *p<0.01, ***p<0.001).

(C) Mean brain weight at P180 in mice fed SD or KD (n=8-13 mice).

(D) Mean liver mRNA expression of *Hmgcs2* in P180 mice fed KD relative to SD values with individual data points (n=5 animals per group, Student's t-test, ***p<0.001).
(E) Blood 3HB and glucose in mice treated as in (A) (n= 24-25, 2way ANOVA with Sidak's post test, ***p<0.001).
(F) Glucose tolerance test (GTT) of P180 mice fed KD or SD with quantification of the area under the curve (n=10 animals per group).
(G) - (I) Representative immunoblots for SCOT (G), MCT1 (H), and Glut1 (I) at P180 in cortex of mice fed SD or KD with quantification of mean relative abundance with individual data points. Reprobing for actin confirmed equal protein loading (n=5 mice).
(J) Representative immunostainings of cortical sections from P180 mice fed KD or SD detecting astrocytes (S100b) or mature oligodendrocytes (CAII) with quantification (n=5 mice per group). Equal density of glial cells suggests absence of damage induced by long-term KD feeding. Nuclei are stained with DAPI (blue).
(K) Representative co-immunostaining of cortical sections from P180 mice fed KD or SD detecting MCT1 and endothelial cells (CD31) with quantification of mean MCT1 fluorescence per CD31 area (n=4-5 mice per group). Nuclei are stained with DAPI (blue).
(L) Representative co-immunostaining of cortical sections from P180 mice fed KD or SD detecting neurons (NeuN) and microglia (Iba1) with quantification of mean cells per area (n=3-5 mice per group). Nuclei are stained with DAPI (blue).
All scales, 50 µm.

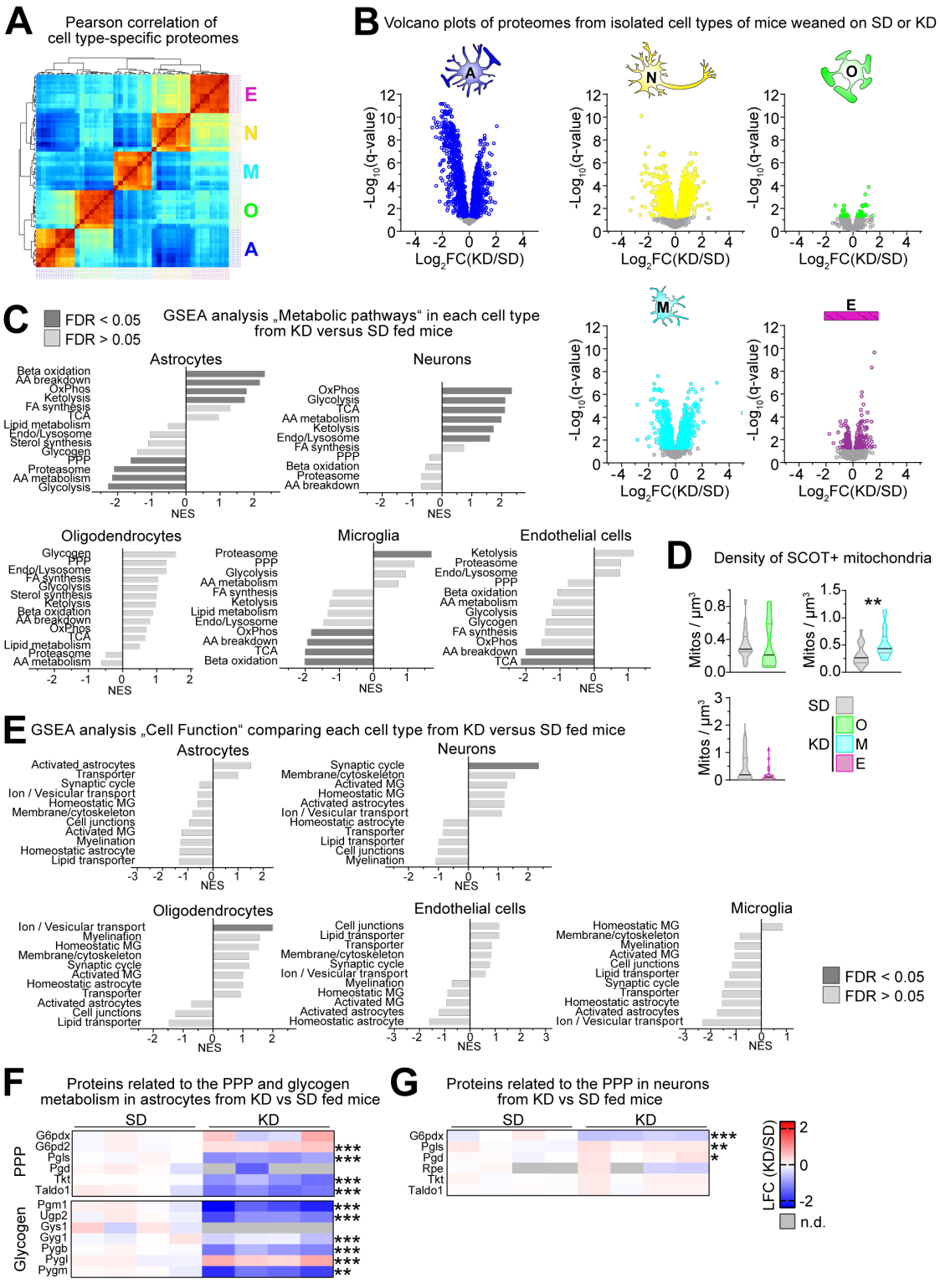

Fig. S4.

Proteome analysis of isolated cell types from mice fed SD or KD

(A) Pearson correlation of cell type-specific proteome data sets obtained from SD or KD-fed mice at P42.

(B) Volcano plots of astrocyte, neuron, oligodendrocyte, microglia, and endothelial cell fractions isolated from P42 mice fed SD versus KD. Colored circles represent proteins with significant abundance changes q-mod<0.05. Number of quantified proteins were

as follows (average sequence coverage in parentheses): A 2297 (38.4%), N 2507 (42.8%), O 1797 (34.8%), M 2221 (35.8%), E 2405 (39.8%).

(C) Normalized enrichment scores (NES) of metabolic pathways by GSEA, comparing LFC of cell type-specific proteomes from P42 mice fed KD versus SD.

(D) Median density of SCOT+ mitochondria ± interquartile range per cell soma volume in endothelial cells, oligodendrocytes, and microglia of mice fed SD or KD (Mann-Whitney test, **$p<0.01$).

(E) Normalized enrichment scores (NES) of cell function processes by GSEA, comparing LFC of cell type-specific proteomes from P42 mice fed KD versus SD.

(F) Heatmap of proteins related to the PPP and to glycogen metabolism in astrocytes isolated from KD or SD-fed mice (each square represents one animal).

(G) Heatmap of proteins related to the PPP in neurons isolated from KD or SD-fed mice (each square represents one animal). N.d. not detected.

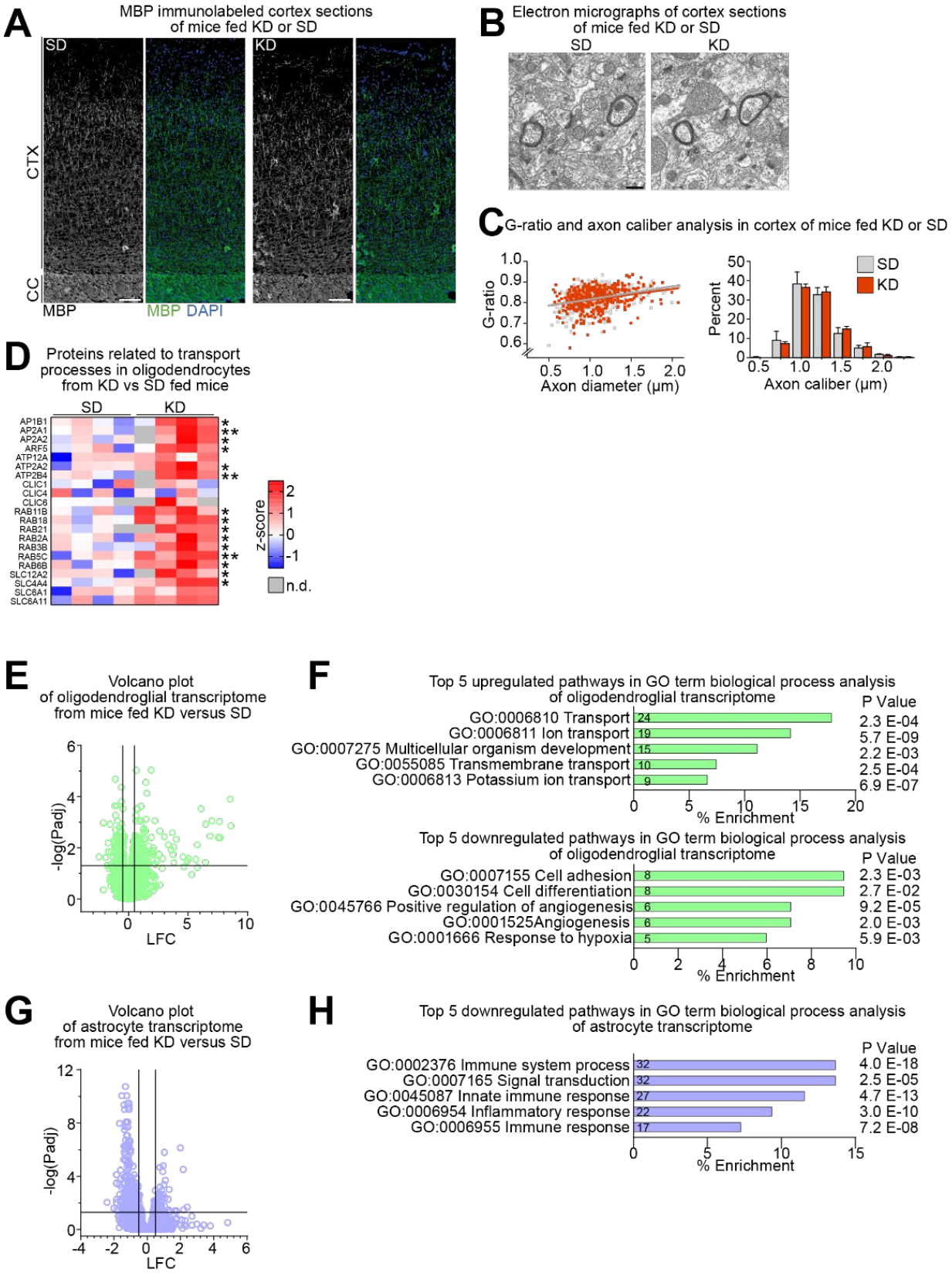

Fig. S5.

Transcriptome profiles in isolated cell types from mice fed SD or KD

(A) Representative images of MBP immunolabeling of brain sections from mice fed KD or SD. Nuclei were stained with DAPI (CC, corpus callosum, CTX, cortex, scale 100 µm).

(B) Representative electron micrograph of cortex sections from mice fed KD or SD (scale, 500 nm).
(C) G-ratio and axon caliber analysis from mice fed KD or SD determined from electron micrographs as in (B) (n=3).
(D) Heatmap of proteins related to ion transport in oligodendrocytes isolated from KD or SD-fed mice (each square represents one animal). N.d. not detected.
(E) Volcano plot of gene expression profiles by RNAseq analysis of isolated oligodendrocytes from mice fed KD versus SD. 13940 genes were identified, 142 genes were significantly upregulated, 88 downregulated (LFC>0.5; padj<0.05). Lines mark the significance thresholds.
(F) David analysis of GO pathways (GO_BP direct terms) of upregulated and downregulated genes in oligodendrocytes of the RNAseq analysis in (E). Percent enrichment reflects the percent of genes that were differentially regulated in the transcriptome that belong to the respective pathway. Numbers in the bars represent the number of associated genes.
(G) Volcano plot of gene expression profiles by RNAseq ansalysis of isolated astrocytes from mice fed KD versus SD. 14683 genes were identified, 20 genes were significantly upregulated, 160 downregulated (LFC>0.5; padj<0.05). Lines mark the significance thresholds.
(H) David analysis of GO pathways (GO_BP direct terms) of downregulated genes in astrocytes of the RNAseq analysis in (G). Percent enrichment reflects the percent of genes that were differentially regulated in the transcriptome that belong to the respective pathway. Numbers in the bars represent the number of associated genes. Upregulated pathways (containing at least 5 genes) were not identified.

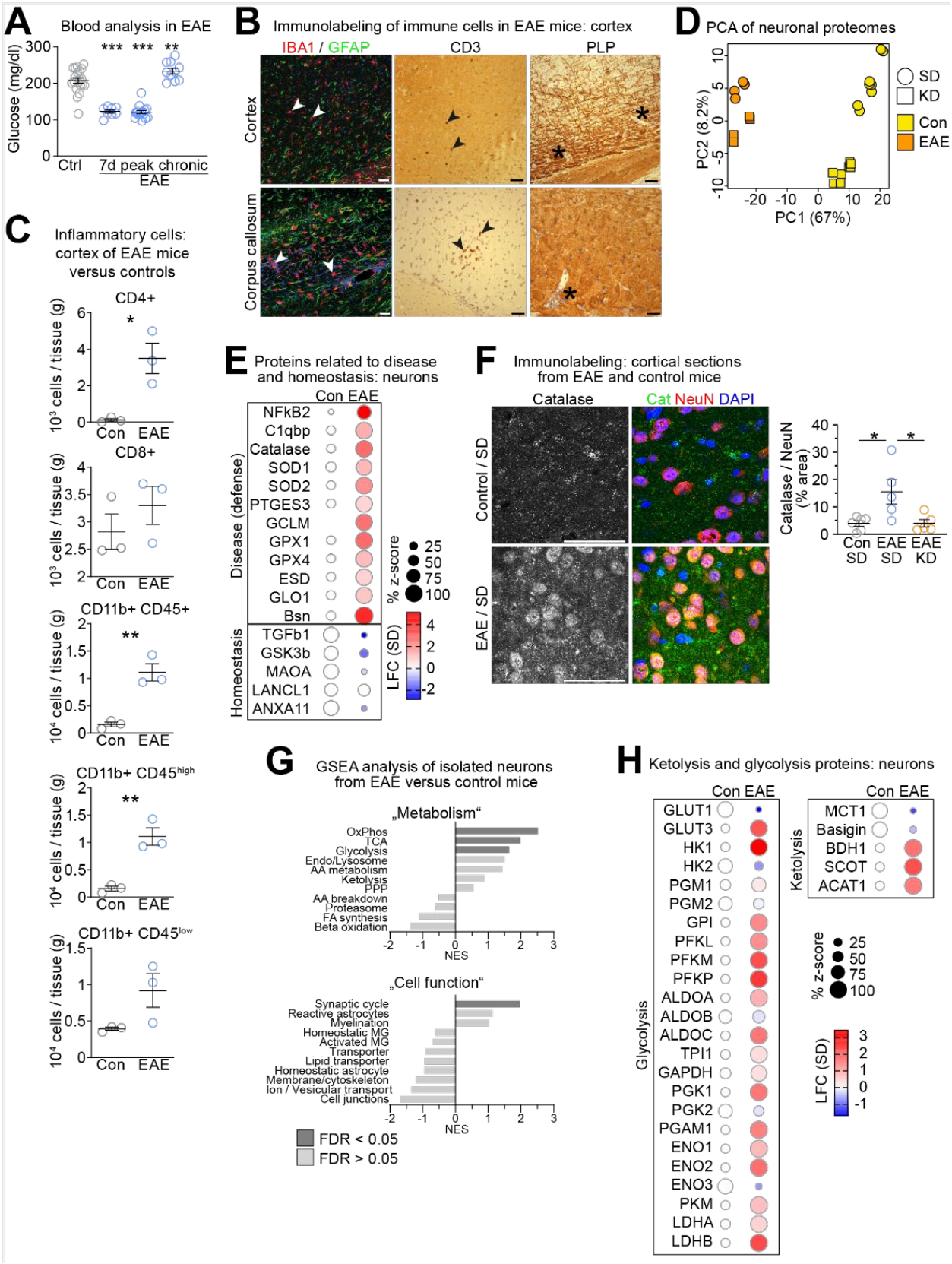

Fig. S6.

EAE disease in the cerebral cortex

(A) Blood glucose levels in EAE and control mice. (n=8-16 mice; 1way ANOVA with Dunnet's post test for comparisons to SD-fed control mice).

(B) Representative images of demyelinating disease in the cortex and corpus callosum of EAE mice. Gliosis is shown by co-immunolabeling of GFAP (astrogliosis) and Iba1 (microgliosis, white arrowheads point to microglia with activated morphology). CD3 labels infiltrating T cells (black arrowheads). Demyelinated lesions with infiltrating cells are marked by the absence of MBP signal (asterisks).
(C) Mean density of inflammatory cells ± SEM in the cortex of EAE mice compared to untreated controls analyzed by flow cytometry (n=3 mice; unpaired two-sided Student's t-test).
(D) PCA of neuronal proteomes from cortex of EAE and control mice at the peak of disease fed SD or KD. Calculation was based on complete cases (i.e. proteins quantified in each replicate of all cell types; 947 out of 3913 proteins in total) to prevent potential clustering effects of missing values.
(E) Bubble plot of disease defense and homeostatic markers in cortical neurons from EAE mice and controls.
(F) Catalase and NeuN immunolabeling of cortical sections with quantification (n=5-6 mice; 1way ANOVA with Tukey's post test).
(G) GSEA 'metabolism' and 'cell function' comparing neuronal profiles from EAE versus control mice at the peak of disease.
(H) Bubble plot of proteins related to glycolysis in cortical neurons isolated from EAE mice versus controls.

*p<0.05, **p<0.001, ***p<0.001, scales 50 µm

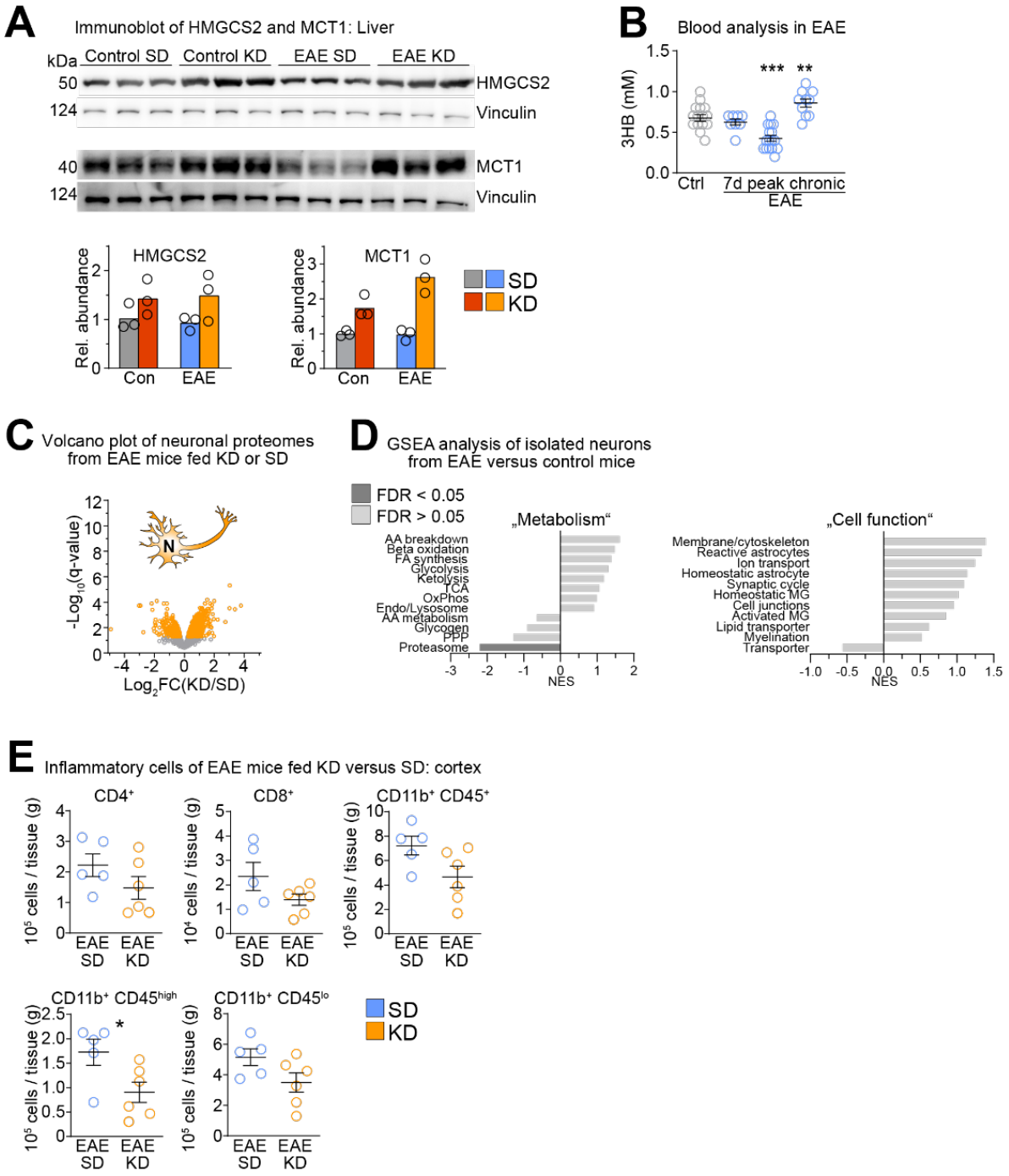

Fig. S7.

Ketogenic diet ameliorates EAE pathology

(A) Immunoblot of HMGCS2 and MCT1 in liver of EAE mice and controls fed KD or SD with quantification relative to Vinculin signals below (n=3 mice).

(B) Blood 3HB levels in EAE and control mice. (n=8-16 mice; 1way ANOVA with Dunnet's post test for comparisons to SD-fed control mice).

(C) Volcano plot of proteomes from cortical neurons from EAE mice fed KD versus SD.

(D) GSEA 'metabolism' and 'cell function' comparing neuronal profiles from EAE mice fed KD versus SD.

(E) Mean density of inflammatory cells ± SEM in the cortex of EAE mice fed KD or SD analyzed by flow cytometry (n=5-6 mice; unpaired two-sided Student's t-test; *p<0.05).

Data table S1. (separate file)

Label-free quantification of proteins in isolated cortical cell types

Identification and quantification data of proteins detected by ion mobility-enhanced DIA-MS (UDMSe). Four animals each for the different age/diet conditions (P14, P42_SD, P42_KD) were processed as biological replicates with a technical replicate at data acquisition level (double injection), resulting in a total of 24 LC-MS runs per cell type. EAE neurons were from two animals each at two different diets (P42_SD, P42_KD), resulting in a total of 8 LC-MS runs per condition. Proteins (FDR < 1%; 2 peptides/protein, one unique) and peptides (FDR < 1%; ≥6 amino acids) were identified by database search against the UniprotKB/SwissProt mouse database using PLGS. Data were post-processed with the software package ISOQuant to calculate absolute in-sample amounts for each detected protein based on the TOP3 approach. Reported abundance values are defined as the relative amount of each protein in respect to the sum over all detected proteins (ppm: parts per million (w/w) of total protein). Typical contaminant proteins like keratins were filtered. Significant changes in protein abundance were detected by moderated t-statistics using a limma-based data analysis pipeline in R (see Materials & Methods for details). No imputation of missing values was performed.

Data table S2. (separate file)

Gene sets 'Cell function'

Custom-select list of genes used for GSEA of cell function processes.

Data table S3. (separate file)

Gene sets 'Metabolic pathways'

Custom-select list of genes used for GSEA of metabolic pathway.

Data table S4. (separate file)

Targeted expression profile in liver from P42 mice fed KD versus SD

Gene expression in liver lysates from KD- versus SD-fed animals at P42.

Data table S5. (separate file)

Targeted expression profile in cortex from P42 mice fed KD versus SD

Gene expression in cortex lysates from KD- versus SD-fed animals at P42.

Data table S6. (separate file)

Metabolomic analysis in cortex from P42 mice fed KD versus SD

Metabolomic profile determined by GC/MS of cortex samples from P42 mice fed KD or SD showing log2 fold changes and adjusted p values.

Data table S7. (separate file)

Transcriptome of isolated oligodendrocytes from mice fed KD versus SD

Data table S8. (separate file)

Transcriptome of isolated astrocytes from mice fed KD versus SD

Data table S9. (separate file)
Mitochondrial carrier abundance mice fed KD versus SD
Log2 fold change (LFC) and adjusted q-mod values of proteins related to mitochondrial carriers in isolated cells from KD- versus SD-fed animals.

Data table S10. (separate file)
Targeted expression profile in liver from EAE mice fed KD versus SD
Gene expression in liver lysates from KD- versus SD-fed EAE animals at the peak of the disease.

Data table S11. (separate file)
Primer sequences used for expression analysis
All primer used for expression analysis were intron-spanning (3'-5').

Movie S1. (separate file)
Representative movie of ALDH1L1+ astrocytes with SCOT+ mitochondria of SD and KD fed mice
3D reconstructions of ALDH1L1+ astrocytes (green), nuclear staining (blue) and SCOT + mitochondria in SD and KD fed mice. Blowup of astrocyte process surface area including SCOT+ surface area.